



Original article

β -elemene promotes miR-127-3p maturation, induces NSCLCs autophagy, and enhances macrophage M1 polarization through exosomal communication

Xiahui Wu ^{a, b, 1}, Jie Wu ^{c, 1}, Tingting Dai ^{d, 1}, Qiangcheng Wang ^e, Shengjie Cai ^f,
Xuehan Wei ^f, Jing Chen ^{g, *}, Ziyu Jiang ^{a, b, **}

^a Department of Oncology, Lianyungang Integrated Traditional Chinese and Western Medicine Clinical College, Nanjing University of Chinese Medicine, Nanjing, 222002, China

^b Department of Oncology, The First People's Hospital of Lianyungang, Lianyungang, Jiangsu, 222002, China

^c Department of Digestive System, Pukou Hospital of Traditional Chinese Medicine, Nanjing, 210000, China

^d Department of Oncology, Jinling Hospital, School of Medicine, Nanjing University, Nanjing, 210000, China

^e Department of Oncology, the Affiliated Cancer Hospital of Nanjing Medical University & Jiangsu Cancer Hospital & Jiangsu Institute of Cancer Research, Nanjing, 210000, China

^f The Third Clinical Medical College, Nanjing University of Chinese Medicine, Nanjing, 210028, China

^g Department of Biochemistry and Molecular Biology, School of Medicine, Nanjing University of Chinese Medicine, Nanjing, 210023, China



ARTICLE INFO

Article history:

Received 19 October 2023

Received in revised form

29 January 2024

Accepted 6 March 2024

Available online 8 March 2024

Keywords:

β -elemene

miR-127-3p

NSCLC

Akt/mTOR/p70S6K

MAPK4

ABSTRACT

β -elemene has been observed to exert inhibitory effects on a multitude of tumors, primarily through multiple pathways such as the inhibition of cancer cell proliferation and the induction of apoptosis. The present study is designed to elucidate the role and underlying mechanisms of β -elemene in the therapeutic intervention of non-small cell lung cancer (NSCLC). Both *in vitro* and *in vivo* experimental models corroborate the inhibitory potency of β -elemene on NSCLCs. Our findings indicate that β -elemene facilitates the maturation of miR-127-3p by inhibiting CBX8. Functioning as an upstream regulator of MAPK4, miR-127-3p deactivates the Akt/mTOR/p70S6K pathway by targeting MAPK4, thereby inducing autophagy in NSCLCs. Additionally, β -elemene augments the packaging of miR-127-3p into exosomes via SYNCRIP. Exosomal miR-127-3p further stimulates M1 polarization of macrophages by suppressing ZC3H4. Taken together, the detailed understanding of the mechanisms through which β -elemene induces autophagy in NSCLCs and facilitates M1 polarization of macrophages provides compelling scientific evidence supporting its potential utility in NSCLC treatment.

© 2024 The Authors. Published by Elsevier B.V. on behalf of Xi'an Jiaotong University. This is an open access article under the CC BY-NC-ND license (<http://creativecommons.org/licenses/by-nc-nd/4.0/>).

1. Introduction

Lung cancer remains a significant global health burden, with an alarming annual diagnosis of 2 million new cases worldwide [1–3]. Alarmingly, Asia contributes to half of these cases [4,5], with China bearing a significant proportion where lung cancer consistently ranks first in incidence and mortality among men, and second in

incidence but first in mortality among women [3,4]. Non-small cell lung cancer (NSCLC), the predominant subtype of lung cancer, accounts for over 80% of all cases. Despite advancements in diagnostic and therapeutic strategies, the prognosis of NSCLC patients remains suboptimal.

Traditional Chinese medicine, renowned for its ability to regulate homeostasis, mitigate toxicity, and enhance efficacy, offers unique therapeutic potential in lung cancer management [6]. One such medicinal plant, Curcuma wenyujin, is commonly employed in the clinical treatment of solid tumors [7]. β -elemene, the principal component extracted from Curcuma wenyujin, has demonstrated inhibitory effects on several tumors, including lung cancer, through mechanisms such as inducing protective autophagy, inhibiting proliferation, inducing apoptosis, and arresting the cell cycle. With its reduced toxicity compared to cytotoxic drugs and efficacy in

* Corresponding author.

** Corresponding author. Department of Oncology, Lianyungang Integrated Traditional Chinese and Western Medicine Clinical College, Nanjing University of Chinese Medicine, Nanjing, 222002, China.

E-mail addresses: chenjing91@outlook.com, dr_chenjing@njucm.edu.cn (J. Chen), 770020240001@xzhmu.edu.cn (Z. Jiang).

¹ These authors contributed equally to this work.

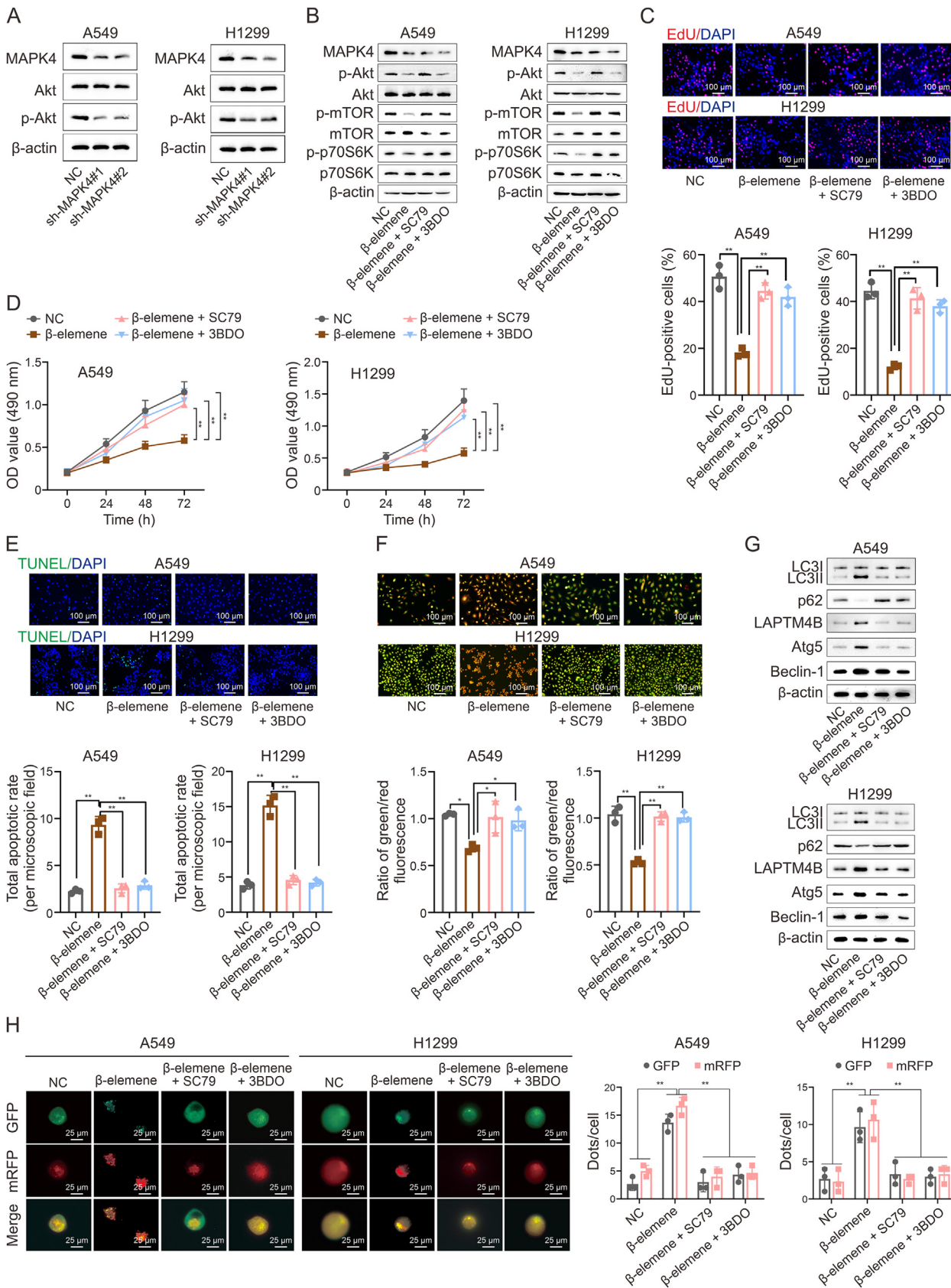


Fig. 1. β-elemene inhibits mitogen-activated protein kinase (MAPK)/Akt pathway to induce autophagy and apoptosis, and suppress proliferation in non-small cell lung cancer cells (NSCLCs). (A) The expression levels of MAPK4, Akt, and p-Akt in A549 and H1299 cells treated with sh-negative control (NC) or sh-MAPK4 were analyzed by Western blot. (B) Western blot showed the effects of β-elemene on key factors of MAPK4 and Akt/mTOR pathways. (C, D) Proliferation levels of NSCLCs in different treatment groups measured by 5-Ethynyl-2'-deoxyuridine (EdU) (C) and cell counting kit 8 (CCK8) (D) assays. (E, F) Apoptosis levels of NSCLCs detected by TdT-mediated dUTP nick end labeling (TUNEL) (E) and

controlling ascites, β -elemene presents a promising avenue for cancer treatment [8,9].

The role of autophagy in cancer progression has been extensively studied and validated [10]. Autophagy exhibits a dual function in tumor development, either inhibiting or promoting tumor growth depending on the tumor type, stage, and genetic background [10,11]. The complex role of autophagy in the progression of several diseases, including NSCLC, is closely linked with microenvironmental stress and immune system status. For instance, autophagy has been implicated in the regulation of NSCLC progression [12,13], making the modulation of autophagy balance a potential therapeutic strategy for NSCLC patients.

Tumorigenesis is profoundly influenced by the tumor microenvironment (TME), with exosomes playing an integral role in mediating communication between tumor cells and stromal cells, thereby modulating various tumor-related behaviors [14]. Exosome-derived microRNAs (miRNAs) regulate multiple biological behaviors of tumors by silencing target genes [15]. As previously established, miR-127-3p functions as an autophagy regulator and tumor suppressor [16–18]. However, its regulatory role in the TME affecting NSCLC growth warrants further exploration.

Macrophages, influenced by different microenvironments, can differentiate into distinct phenotypes and exert diverse biological functions [19]. M1 and M2 macrophages, common macrophage polarization types, display different functions and morphologies [20]. M1 macrophages primarily influence pro-inflammatory processes in the TME and play a crucial role in anti-tumor immunity, whereas M2 macrophages have been implicated in promoting tumor development [21]. Macrophages are indispensable for controlling cancer progression and for immunotherapy.

In summary, this study aims to elucidate the potential mechanisms of β -elemene in inducing autophagy in NSCLCs and promoting M1 polarization of macrophages. It seeks to clarify the role of miR-127-3p in regulating the autophagic pathway to induce autophagy in NSCLCs, and to investigate the impact of exosomal miR-127-3p and its downstream regulatory pathway on M1 polarization of macrophages.

2. Materials and methods

2.1. Cell culture and treatment

The A549 and H1299 cell lines utilized in this study were procured from the Institute of Biochemistry and Cell Biology, Chinese Academy of Sciences (Shanghai, China). The cells were maintained in RPMI-1640 medium (Hyclone, Logan, UT, USA), enriched with 10% fetal bovine serum (Gibco, Carlsbad, CA, USA) and 1% penicillin-streptomycin (Gibco). For experiments involving β -elemene, the culture medium was further fortified with 2 μ g/mL of β -elemene (Jingang Pharmaceutical, Dalian, China). All cell cultures were sustained in a sterile environment at 37 °C with a 5% CO₂ atmosphere.

2.2. Cell transfection

miR-127-3p mimics, inhibitors, and antagomirs, along with the corresponding negative control (NC) mimics, inhibitors, and antagomirs, were sourced from RiboBio (Guangzhou, China). Short hairpin RNAs (shRNAs) targeting SYNCRIP and ZC3H4, and the corresponding negative control (sh-NC), were procured from Bi-run (Wuhan, China). Overexpression vectors for CBX8 and mitogen-

activated protein kinase 4 (MAPK4) were constructed by inserting their respective full-length cDNA into the pcDNA3.1 vector, with the empty pcDNA3.1 vector serving as the control. Cell transfection was carried out using Lipofectamine™ 3000 Transfection Reagent (Thermo Fisher Scientific, New York, NY, USA) following the manufacturer's protocol. The Lentivirus Packaging Kit (GeneChem, Shanghai, China) was employed for *in vivo* experiments.

2.3. Quantitative real-time polymerase chain reaction (RT-qPCR)

The expression levels of RNAs were determined using RT-qPCR. Total RNA was isolated from A549 and H1299 cells using TRIzol reagent (Thermo Fisher Scientific), whereas exosomal RNA was extracted with the ExoQuick® Exosome RNA Column Purification Kit (System Biosciences, Mountain View, CA, USA). The extracted RNA samples were then reverse transcribed into cDNA using the ReverTra Ace qPCR RT Kit (Toyobo, Osaka, Japan). Real-time fluorescence quantitative PCR analysis was conducted using the ABI 7500 Real-time PCR analyzer and SYBR Premix Ex Taq (Takara, Kyoto, Japan). The relative expression of target RNAs was quantified using the 2^{- $\Delta\Delta$ Ct} method, with reduced glyceraldehyde-phosphate dehydrogenase (GAPDH) or U6 serving as the reference gene.

2.4. Western blot analysis

To obtain total cellular protein, cells were lysed on ice for 30 min using radioimmunoprecipitation assay (RIPA) buffer supplemented with protease and phosphatase inhibitors. Protein concentration was determined via the BCA Assay Kit (Pierce, Rockford, IL, USA). Equivalent protein quantities were resolved using 10% sodium dodecyl sulfate-polyacrylamide gel electrophoresis (SDS-PAGE) and transferred to polyvinylidene fluoride (PVDF) membranes (Millipore, Boston, MA, USA). Membranes were blocked with 5% non-fat milk in team-based simulation training (TBST) and incubated overnight at 4 °C with specific primary antibodies (Abcam, Cambridge, UK). This was followed by 1 h incubation at room temperature with appropriate horseradish peroxidase (HRP)-conjugated secondary antibodies (Abcam). Protein bands were visualized using an electrochemiluminescence (ECL) detection system.

2.5. 5-Ethynyl-2'-deoxyuridine (EdU)

To label proliferating NSCLCs, the cells were co-incubated with a 50 μ M EdU reagent (RiboBio) for 2 h, following the manufacturer's instructions. After washing the cells twice with PBS, they were fixed with 4% paraformaldehyde and permeabilized using 0.5% Triton X-100. Subsequently, the cells were stained with Apollo and Hoechst 33342 in the dark for 30 min. Finally, the stained cells were observed using a fluorescence microscope.

2.6. Cell counting kit 8 (CCK8)

The proliferation ability of NSCLCs was assessed using the widely used CCK8 kit (Beyotime, Shanghai, China). Cells were cultured in a 96-well plate for 24, 48, and 72 h, followed by co-incubation with 20 μ L of CCK8 reagent at 37 °C for 4 h. The optical density (OD) values were measured at a wavelength of 450 nm.

acridine orange/ethidium bromide (AO/EB) (F) staining. Scale bar = 100 μ m. (G, H) Autophagy levels of NSCLCs measured by Western blot (G) and autophagic flow (H) experiments. Figs. 1B–H examined the effects of β -elemene on the function of NSCLCs, with the same treatments applied to A549 and H1299 cells: dimethyl sulfoxide (DMSO, NC), β -elemene, β -elemene + SC79, and β -elemene+3BDO. ***P* < 0.01.

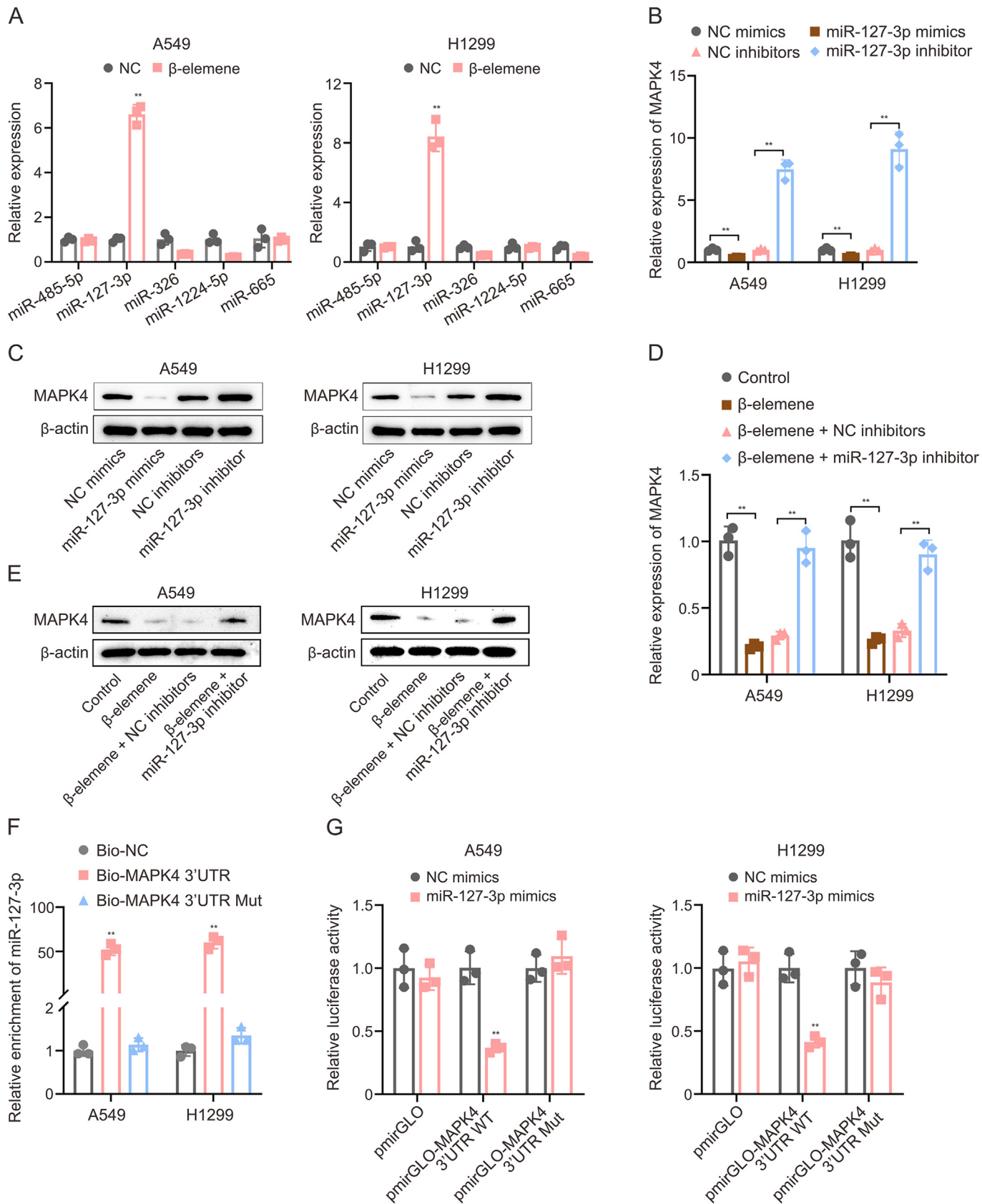


Fig. 2. β-elementine downregulates mitogen-activated protein kinase 4 (MAPK4) by upregulating miR-127-3p. (A) Quantitative real-time polymerase chain reaction (RT-qPCR) was performed to detect 5 candidate miRNAs and screen for upstream regulatory factors of MAPK4 in A549 and H1299 cells treated with dimethyl sulfoxide (DMSO) or β-elementine. (B, C) Changes in MAPK4 mRNA levels and protein expression were analyzed by RT-qPCR (B) and Western blot (C) after overexpression or inhibition of miR-127-3p in A549 and H1299 cells. (D, E) Differential expression of MAPK4 mRNA levels and protein expression were analyzed by RT-qPCR (D) and Western blot (E) after inhibition of miR-127-3p in A549

2.7. TdT-mediated dUTP nick end labeling (TUNEL)

The One Step TUNEL Apoptosis Assay Kit (Beyotime) was employed to label apoptotic cells. 4',6-diamidino-2-phenylindole (DAPI; Thermo Fisher Scientific) was used to label the nuclei. Subsequently, the positive cells were observed under a fluorescence microscope, and the apoptosis rate was analyzed.

2.8. Acridine orange/ethidium bromide (AO/EB) staining

After co-culturing A549 or H1299 cells with β -elemene on 6-well plates for 24 h, the cell suspension was mixed with AO/EB (SenBeijia Biological Technology, Nanjing, China) solution according to the manufacturer's instructions and incubated for 15 min. The morphology of different cells was then observed under a fluorescence microscope.

2.9. mCherry-GFP-LC3 double fluorescence system

Following treatment with mCherry-GFP-LC3, NSCLCs were incubated with the appropriate viral suspension at 37 °C. Transfection was performed after 72 h of culture, followed by a 2-h amino acid deprivation treatment. The autophagy process was monitored under a fluorescence microscope. Red, green, or yellow puncta represented autophagolysosome (mCherry), LC3 puncta, and autophagosome (mCherry + GFP), respectively.

2.10. Dual luciferase reporter assay

The pmirGLO-MAPK4-WT vector was constructed by inserting the MAPK4 3'UTR sequence, which contains the binding site for miR-127-3p, into the reporter plasmid pmirGLO. Similarly, the MAPK4 3'UTR mutant sequence, which lacks the miR-127-3p binding site, was inserted into the pmirGLO vector to create the pmirGLO-MAPK4-Mut vector. The constructed vectors were co-transfected into cells with either miR-127-3p mimics or NC mimics, and the luciferase activity was analyzed using a dual luciferase reporter assay system.

2.11. RNA immunoprecipitation (RIP) assay

The EZ-Magna RIP™ RNA-Binding Protein Immunoprecipitation Kit (Millipore) was used to perform the RIP experiment. Lysates were obtained by incubating NSCLCs or exosomes in a lysis buffer supplemented with protease inhibitors and RNase inhibitors. Subsequently, the lysates underwent immunoprecipitation using magnetic beads conjugated with specific antibodies against Drosha, DICER, SYNCRIP, CBX8, and other proteins. After digestion with proteinase K, the enrichment levels of pri-miR-127, pre-miR-127, or miR-127-3p were assessed using RT-qPCR.

2.12. RNA pulldown assay

The RNA pulldown experiments were conducted following the protocol provided by the manufacturer of the Pierce™ Magnetic RNA-Protein Pull-Down Kit (Thermo Fisher Scientific). Biotinylated miR-127-3p and pre-miR-127 were synthesized by Thermo Fisher Scientific. To analyze the proteins that interacted with the RNA, the pulldown products were subjected to either mass spectrometry analysis or Western blot experiments.

2.13. Fluorescence in situ hybridization (FISH) assay

The colocalization of CBX8 with pre-miR-127 in NSCLCs was assessed using the Fluorescence In Situ Hybridization (FISH) Kit from Ribobio. A549 and H1299 cells were fixed and permeabilized before being incubated with specific FISH probes targeting CBX8 or pre-miR-127. To visualize the cell nuclei, DAPI staining was performed. Subsequently, fluorescence microscopy was used to capture images of the cells.

2.14. Flow cytometry

The expression of CD86-APC (Caprico Biosciences, Atlanta, GA, USA) on the surface of macrophages was quantified using flow cytometry. A total of 100,000 viable cells were collected and washed with 1 × PBS. Subsequently, the cells were stained with 5 μ L of CD86 antibody in a 50 μ L volume of fluorescence-activated cell sorting (FACS) staining buffer. After a 15-min incubation in the dark at 4 °C, the cells were washed with 1 × PBS and resuspended in 400 μ L of FACS staining buffer. Finally, the samples were analyzed using a FACS Symphony A3 flow cytometer (BD Biosciences, San Jose, CA, USA) to determine the proportion of CD86-positive cells.

2.15. Nucleoplasmic separation assay

Total RNA was isolated from NSCLCs using Trizol reagent (Invitrogen, Carlsbad, CA, USA), and nuclear/cytosol fractionation assays were conducted using the nuclear/cytosol fractionation kit (Solarbio, Beijing, China) following the manufacturer's instructions.

2.16. Exosome extraction and identification

Exosome isolation was performed following previously established protocols [22]. Following extraction, the morphology of the exosomes was visualized using transmission electron microscopy. Nanoparticle tracking analysis (NTA) was employed to determine the size distribution of the exosomes. The presence of specific surface markers was confirmed by conducting Western blot analysis.

2.17. Fluorescence labeling and tracing of exosomes

To investigate the mechanism of exosome transfer to recipient cells, DiO cell-labeling solution (Thermo Fisher Scientific) was used to fluorescently label exosomes. After labeling, the exosomes were co-cultured with macrophages. At various time points of co-culture (0, 1, 2, 4, 6, 12, 24, or 48 h), the cells were fixed using a 4% paraformaldehyde solution and permeabilized with 0.01% Triton X-100. The cell cytoskeleton was stained using tetramethylrhodamine isothiocyanate (TRITC; Thermo Fisher Scientific), while the nuclei were counterstained with DAPI. The uptake of exosomes was visualized using a Leica DMi8 inverted microscope equipped with LAX software, and the proportion of DiO-positive cells was quantified.

2.18. In vivo tumorigenic assay

Animal research was conducted following approved animal care guidelines by the ethic committee of Nanjing Medical University (Approval number: 2019LWKYS-009). cMale BALB/c nude mice (6-week-old) were purchased from Charles River Laboratories Research Model Service (Beijing, China) and maintained in a specific pathogen-free environment for 7 days prior to the experiment.

and H1299 cells treated with β -elemene. (F) RNA pulldown was performed to validate the binding of miR-127-3p and MAPK4 3'UTR in A549 and H1299 cells. (G) Luciferase reporter assay confirmed the binding effect of miR-127-3p and MAPK4 3'UTR. ** $P < 0.01$.

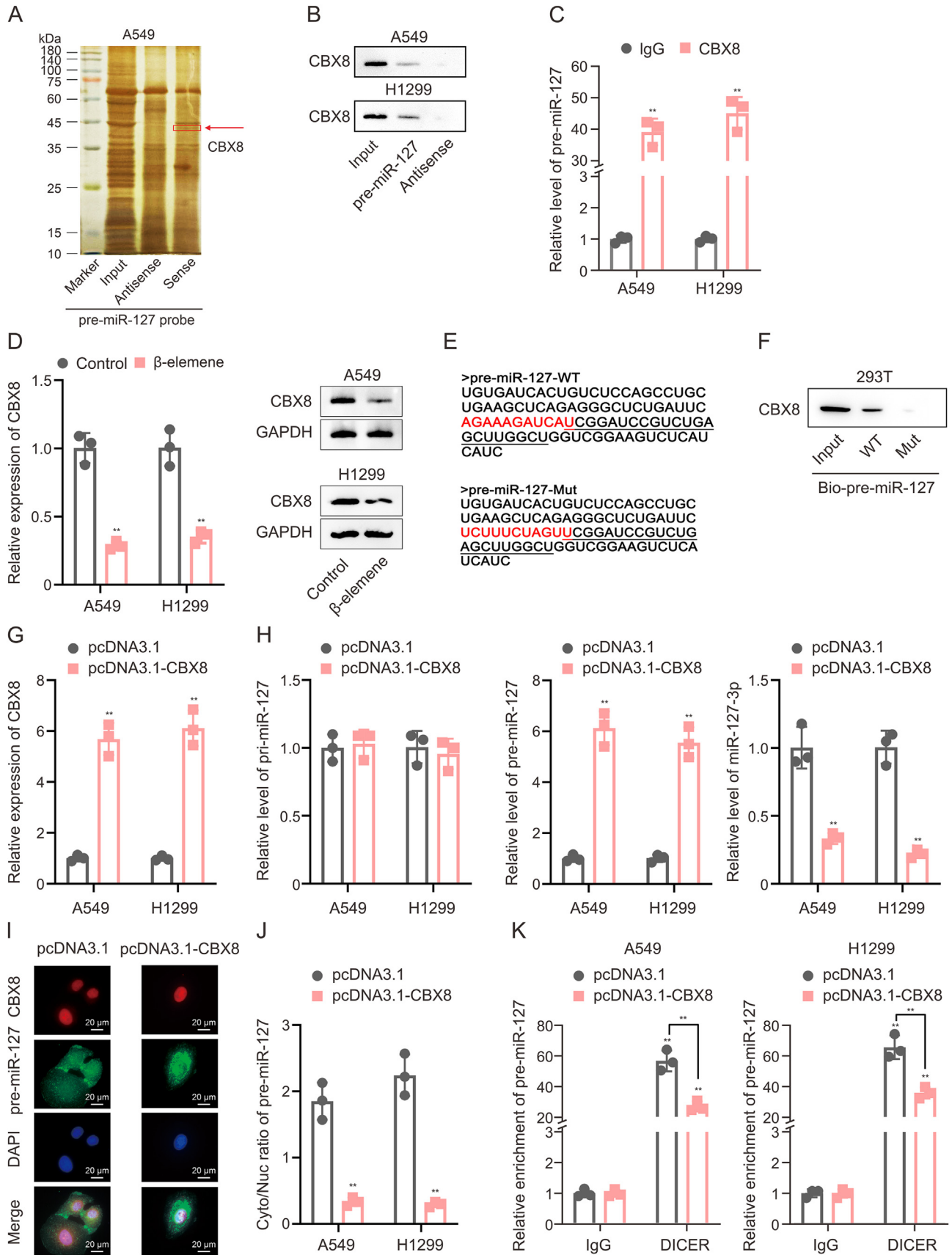


Fig. 3. β-elemene inhibits CBX8 expression and promotes the formation of mature miR-127-3p. (A) Mass spectrometry evaluated the proteins recruited by pre-miR-127 in A549 cells after RNA pull-down and visualized using silver staining. (B) RNA pull-down assays were performed in A549 and H1299 cells to pull down CBX8 and Western blot was used to detect the binding of CBX8 to pre-miR-127. (C) Binding of CBX8 to pre-miR-127 was verified by RNA immunoprecipitation (RIP) assay in A549 and H1299 cells. (D) Expression of

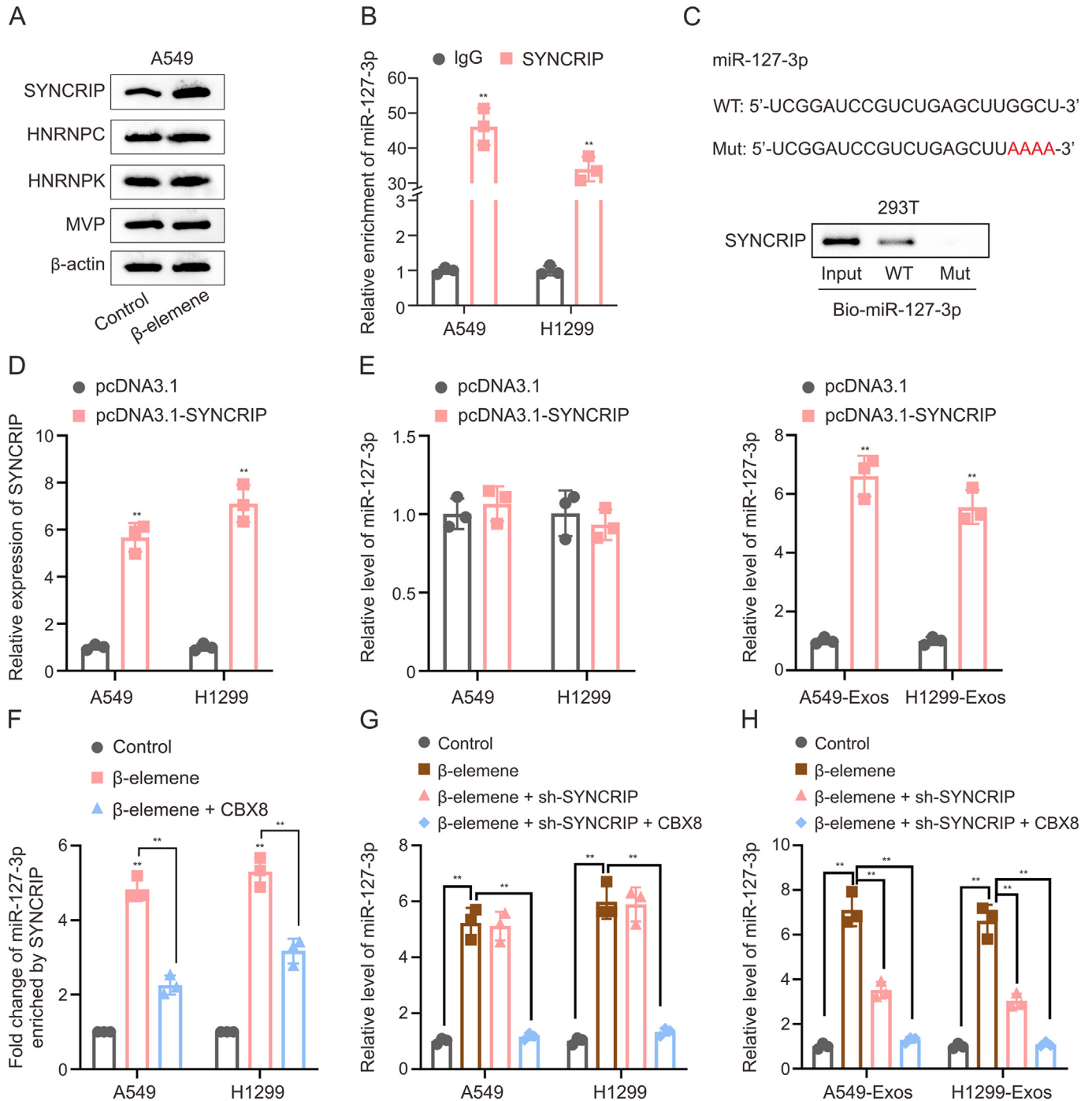


Fig. 4. β-elemene upregulates SYNCRIP to promote the entry of miR-127-3p into exosomes. (A) Expression of HNRNPC, HNRNPK, MVP, and SYNCRIP was detected by Western blot in A549 cells after treatment with dimethyl sulfoxide (DMSO) or β-elemene. (B) RNA immunoprecipitation (RIP) assay was performed in A549 cells and H1299 cells to detect and reveal the binding relationship between miR-127-3p and SYNCRIP. (C) Wild-type (WT) and mutant (Mut) sequences of miR-127-3p were used, and their binding to SYNCRIP was detected using RNA pull-down. (D) Quantitative real-time polymerase chain reaction (RT-qPCR) was used to detect the overexpression efficiency of SYNCRIP in A549 cells and H1299 cells. (E) After SYNCRIP overexpression, RT-qPCR was performed to detect the expression of miR-127-3p in the cells as well as in the corresponding exosomes. (F) RIP assay was performed to detect the changes in the binding between SYNCRIP and miR-127-3p after treatment with β-elemene or simultaneous overexpression of CBX8. (G, H) Expression of miR-127-3p in A549 and H1299 cells (G) and corresponding exosomes (H) was examined by RT-qPCR after different treatments of DMSO, β-elemene, β-elemene + sh-SYCRIP or β-elemene + sh-SYCRIP + CBX8, respectively. ***P* < 0.01.

CBX8 was detected by quantitative real-time polymerase chain reaction (RT-qPCR) in A549 and H1299 cells after treatment with dimethyl sulfoxide (DMSO) or β-elemene. (E) Pre-miR-127 sequence with or without CBX8 binding sites (pre-miR-127-WT or pre-miR-127-Mut). (F) RNA pull-down and Western blot detected the binding relationship between pre-miR-127-WT/Mut and CBX8. (G) RT-qPCR detected the overexpression efficiency of CBX8 in A549 cells and H1299 cells. (H) RT-qPCR detected the expression of pre-miR-127, pre-miR-127 and miR-127-3p in A549 cells and H1299 cells transfected with or without CBX8. (I) Fluorescence *in situ* hybridization (FISH) examined the effect of CBX8 overexpression on the co-localization of CBX8 and pre-miR-127. Scale bar = 25 μm. (J) Nucleoplasmic separation assay detected the effect of CBX8 overexpression on the subcellular distribution of pre-miR-127 in A549 cells and H1299 cells. (K) After overexpression of CBX8 in A549 cells and H1299 cells, RIP experiment was used to analyze the binding between pre-miR-127 and DICER. DAPI: 4',6-diamidino-2-phenylindole. ***P* < 0.01, ****P* < 0.001.

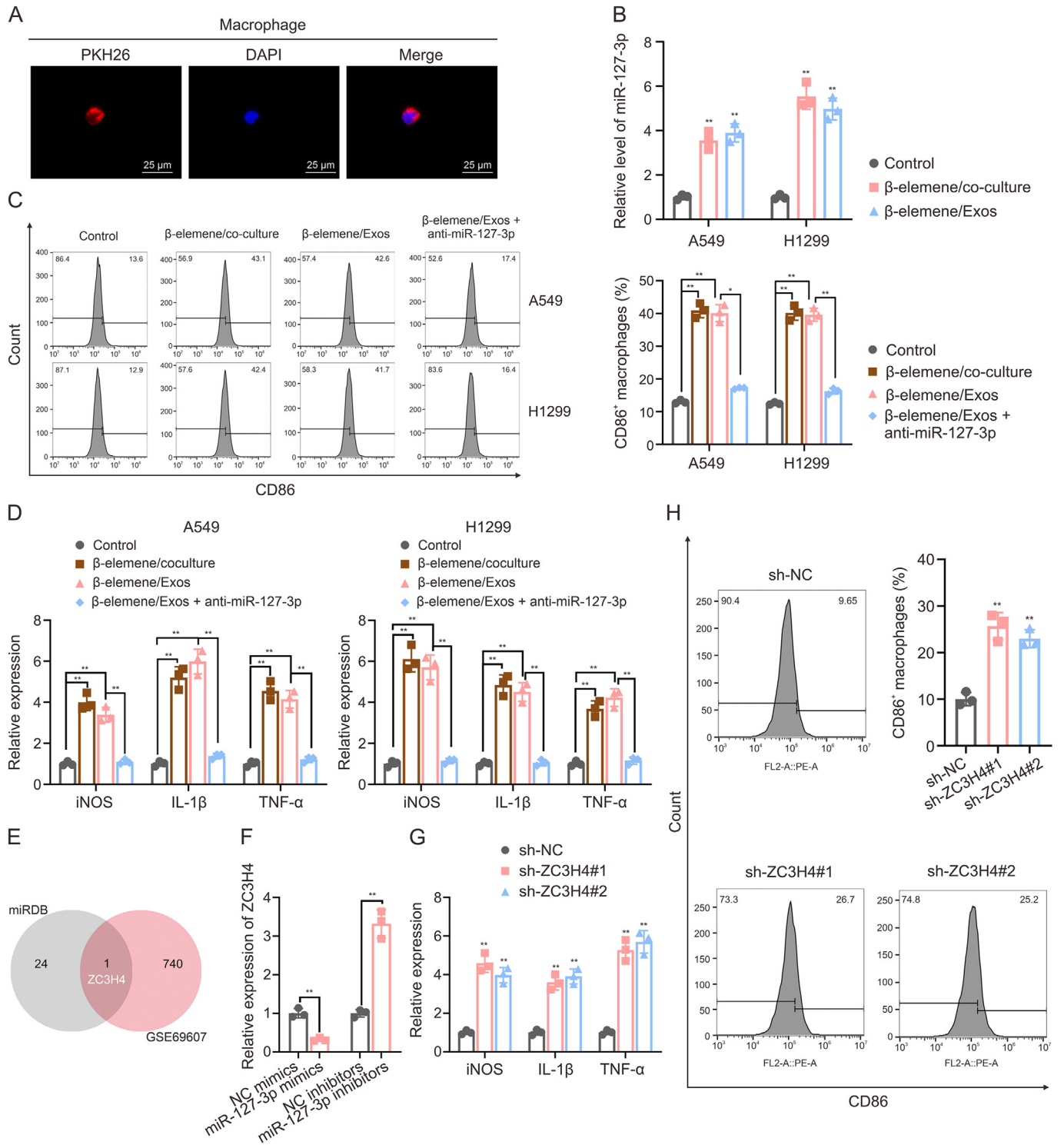


Fig. 5. β -elemene-induced exosomal miR-127-3p promotes macrophage M1 polarization. (A) PKH26 staining traces the uptake of exosomes by macrophages. Red: A549 exosomes stained with PKH26, Blue: Macrophage nuclei stained with 4',6'-diamidino-2-phenylindole (DAPI). (B) Quantitative real-time polymerase chain reaction (RT-qPCR) was used to detect the expression difference of miR-127-3p in different groups of macrophages. (C) Flow cytometry was used to detect the expression of CD86-positive cells in different co-culture groups of macrophages. (D) RT-qPCR was used to detect the expression of M1 polarization markers inducible nitric oxide synthase (iNOS), interleukin-1 β (IL-1 β), and tumour necrosis factor- α (TNF- α) in macrophages of different sources. (E) Venn diagram showing the potential target genes of miR-127-3p screened out by miRDB together and GSE69607. (F) After interference or overexpression of miR-127-3p, RT-qPCR was used to detect the expression difference of ZC3H4. (G) RT-qPCR was used to detect the effect of ZC3H4 interference on M1 polarization markers. (H) Results of flow cytometry after interference with ZC3H4 demonstrated the change in CD86-positive cell rate. Figs. 5B–D sample profiles involved co-culturing non-small cell lung cancer cells (NSCLCs) treated with Control or β -elemene with macrophages, and co-culturing exosomes derived from β -elemene-treated NSCLCs with macrophages. Additionally, in Figure 5C and D, an antagonist of miR-127-3p was added to these co-cultures. The NSCLCs used were A549 cells or H1299 cells. * $P < 0.05$, ** $P < 0.01$.

The transfected A549 cells were subcultured to achieve stable expression, and single-cell suspensions were prepared with a cell concentration of 2.5×10^6 cells/mL. NSCLC animal models were established by subcutaneously injecting nude mice with 200 μ L of the cell suspension. After four weeks, all mice were euthanized, and the tumors were excised for immunohistochemistry (IHC) staining. For IHC, the tissue samples were fixed, dehydrated, embedded, and sectioned into small sections (4 μ m). These sections were then incubated with specific antibodies such as anti-Ki67, anti-LC3, and anti-CD86. Images were captured using an optical microscope.

2.19. Statistical analysis

The statistical analysis was conducted using the GraphPad Prism software. The data were presented as the mean \pm standard error (SE). For comparisons between two groups, the Student's *t*-test was employed. For comparisons among more than two groups, the one-way analysis of variance (ANOVA) with Tukey's or Dunnett's multiple comparisons test was utilized. In the case of comparisons between groups with multiple time points, the two-way ANOVA with Tukey's multiple comparisons test was employed. The notation n.s. indicates no statistical difference, while **P* < 0.05, ***P* < 0.01, and ****P* < 0.001 indicate statistical significance at the corresponding levels of significance.

3. Results

3.1. β -elemene inactivates the MAPK4/mTOR pathway and stimulates autophagy in NSCLC cells

Previous reports have demonstrated that β -elemene can induce endoplasmic reticulum (ER) stress in lung adenocarcinoma cells, which is closely associated with cellular autophagy [23]. Based on this, we hypothesized that β -elemene may also stimulate autophagy in NSCLCs. To investigate this, we assessed autophagy levels in β -elemene-treated NSCLCs. As expected, we observed significant differences in the expression of autophagy-related proteins (Fig. S1A). Moreover, the autophagy pathway that was previously

suppressed in NSCLCs was reactivated with β -elemene treatment (Figs. S1B and C). In summary, β -elemene significantly inhibited NSCLCs proliferation (Fig. S1D) while concurrently elevating autophagy.

Although β -elemene has been shown to trigger autophagy in NSCLCs, the exact underlying mechanism is still unclear. A previous study has highlighted the critical role of MAPK4 in the MAPK/mTOR autophagy pathway [24], which we have corroborated (Fig. 1A). Building on this, we conducted Western blot to evaluate the impact of β -elemene on MAPK4 and key proteins in the Akt/mTOR/p70S6K pathway (Fig. 1B). We found that MAPK4 expression was significantly downregulated by β -elemene. Furthermore, the phosphorylation levels of Akt, mTOR, and p70S6K were significantly reduced. However, upon the introduction of SC79 (an Akt activator), these reductions were reversed, resulting in an increase in phosphorylation. Interestingly, the phosphorylation level of Akt remained unaffected following treatment with 3BDO (an mTOR activator). These results suggest β -elemene inhibits MAPK4, thereby deactivating Akt/mTOR/p70S6K signaling and inducing autophagy. To validate this, we functionally assayed NSCLCs with the same treatments. We confirmed β -elemene inhibits NSCLCs proliferation, which can be rescued by SC79 or 3BDO co-treatment (Figs. 1C and D). Notably, apoptosis and autophagy levels were inversely associated with proliferation (Figs. 1E–H).

Crucially, β -elemene exerts an inhibition on NSCLCs by deactivating p70S6K, achieved through the reduction of Akt and mTOR phosphorylation levels. Notably, this inhibitory effect is augmented when β -elemene is combined with a p70S6K inhibitor (Figs. S1E and F).

3.2. β -elemene downregulates MAPK4 which could inhibit autophagy in NSCLCs by activating miR-127-3p

Further investigation is warranted to gain a comprehensive understanding of the underlying mechanism by which β -elemene exerts its inhibitory effects on MAPK4 and induces autophagy. To explore the upstream mechanism of β -elemene in inhibiting MAPK4 expression, we employed Targetscan (<https://www.>

Table 1

There are 25 predicted targets for hsa-miR-127-3p in miRDB. MAPK4 and ZC3H4 are key downstream factors in the regulatory effects of β -elemene mediated by miR-127.

Target rank	Target score	Gene symbol	Gene description
1	94	BCCIP	BRCA2 and CDKN1A interacting protein
2	89	KIF3B	Kinesin family member 3B
3	83	ATP1A2	ATPase Na ⁺ /K ⁺ transporting subunit alpha 2
4	83	SYN3	Synapsin III
5	83	MTSS1L	MTSS1L, I-BAR domain containing
6	82	ACO2	Aconitase 2
7	80	EPOP	Elongin BC and polycomb repressive complex 2 associated protein
8	78	AGAP3	ArfGAP with GTPase domain, ankyrin repeat and PH domain 3
9	77	KMT5A	Lysine methyltransferase 5A
10	73	SEPT7	Septin 7
11	70	ZC3H4	Zinc finger CCCH-type containing 4
12	66	BLZF1	Basic leucine zipper nuclear factor 1
13	64	MAPK4	Mitogen-activated protein kinase 4
14	64	FJX1	Four-jointed box kinase 1
15	64	MAG1	Membrane associated guanylate kinase, WW and PDZ domain containing 1
16	61	VAMP2	Vesicle associated membrane protein 2
17	58	NKAIN3	Sodium/potassium transporting ATPase interacting 3
18	57	ATP2B2	ATPase plasma membrane Ca ²⁺ transporting 2
19	56	ZNF3	Zinc finger protein 3
20	55	SLC25A2	Solute carrier family 25 member 2
21	55	TPTE2	Transmembrane phosphoinositide 3-phosphatase and tensin homolog 2
22	53	KLK12	Kallikrein related peptidase 12
23	51	TTC9	Tetratricopeptide repeat domain 9
24	50	PPP1R11	Protein phosphatase 1 regulatory inhibitor subunit 11
25	50	EPM2A	EPM2A, laforin glucan phosphatase

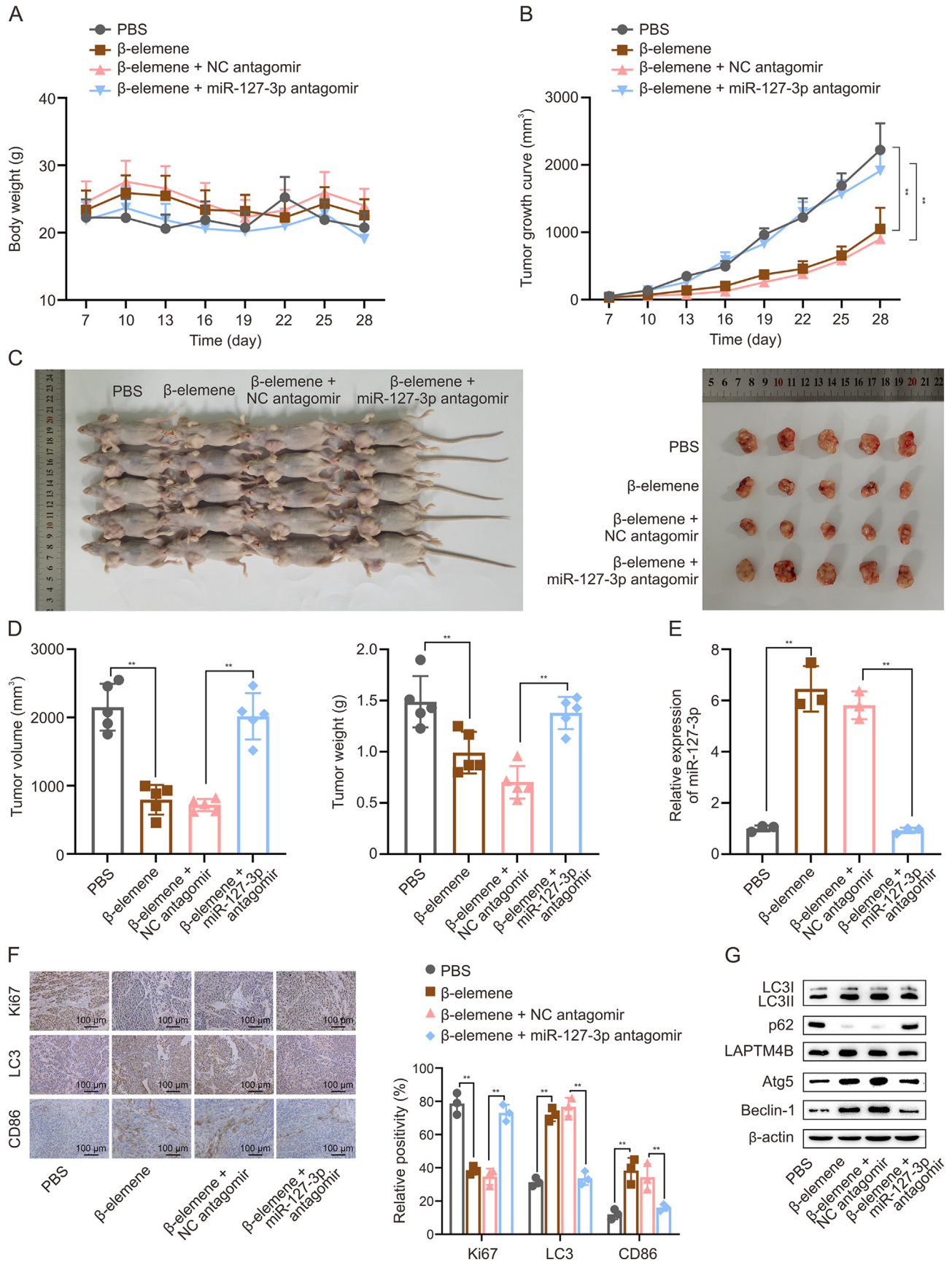


Fig. 6. β-elemene-mediated upregulation of miR-127-3p inhibits non-small cell lung cancer (NSCLC) tumor growth *in vivo*. (A) The curve displayed the changes in body weight of mice in different groups. (B) The growth of transplanted tumors *in vivo* was measured and analyzed in the nude mouse model. (C, D) Images of transplanted tumors in different

targets.org) to identify potential miRNAs that interact with MAPK4. Our analysis identified five potential mammalian miRNAs, namely miR-485-5p, miR-127-3p, miR-326, miR-1224-5p, and miR-665 (Fig. S2A). Among these, only miR-127-3p exhibited a significant increase in NSCLCs upon β -elemene treatment (Fig. 2A). Subsequently, we conducted experiments to examine the impact of transfected miR-127-3p on MAPK4 expression at both the RNA and protein levels. Consistently, augmented miR-127-3p levels resulted in a more pronounced inhibition of MAPK4 expression (Figs. 2B and C). Considering the inhibitory effect of β -elemene on MAPK4 expression, we performed additional experiments by interfering with miR-127-3p in conjunction with β -elemene treatment. Intriguingly, we observed a complete reversal of MAPK4 inhibition (Figs. 2D and E), suggesting that β -elemene regulates MAPK4 through miR-127-3p. Functionally, we evaluated the impact on proliferation, apoptosis, and autophagy levels, and found that the effects of miR-127-3p, whether positive or negative, were counteracted by MFAP4 (Fig. S3). Based on these compelling findings, we have confirmed that MAPK4 is a downstream target of miR-127-3p.

To further elucidate the regulatory role of miR-127-3p on MAPK4, we introduced mutations in the binding region of the MAPK4 3'UTR to disrupt the interaction with miR-127-3p (Fig. S2B). The RNA pulldown assay specifically enriched miR-127-3p using the wild-type probe of MAPK4 3'UTR (Fig. 2F), and the luciferase reporter assay validated the binding relationship between MAPK4 3'UTR and miR-127-3p (Fig. 2G).

In conclusion, β -elemene induces autophagy in NSCLCs by enhancing miR-127-3p and subsequently inhibiting MAPK4.

3.3. β -elemene enables pre-miR-127 to escape from nucleoplasmic translocation restrictions and mature towards miR-127-3p by inhibiting CBX8

To investigate the underlying cause of miR-127-3p upregulation, we conducted an initial study on the effect of β -elemene on its transcriptional function. The luciferase reporter assay results indicated no significant difference in the promoter activity of miR-127-3p precursor gene RTL1 with or without β -elemene treatment (Figs. S4A and B). This suggests that β -elemene does not affect the transcription of miR-127-3p. Therefore, we hypothesized that the differential expression of miR-127-3p occurs after transcription but before maturation. We analyzed the expression of pri-miR-127 and pre-miR-127 in the presence or absence of β -elemene treatment. The expression of pri-miR-127 did not show a significant difference, while the expression of pre-miR-127 was significantly reduced (Fig. S4C), supporting our hypothesis. We also observed no significant change in the binding of pri-miR-127 to Drosha after β -elemene treatment (Fig. S4D). However, the binding of pre-miR-127 to DICER was significantly increased (Fig. S4E), indicating that β -elemene promotes the maturation of pre-miR-127 to miR-127-3p.

Based on the results of the aforementioned experimental analysis, we conducted RNA pulldown and mass spectrometry to identify proteins interacting with pre-miR-127 (Fig. 3A), and CBX8 was identified as the primary target. CBX8 negatively regulates miRNA expression during the processing of pre-miRNA to mature miRNA. It interacts with the precursor miRNA through its own RNA-binding domain and restricts the nucleoplasmic translocation

of pre-miRNA, thus participating in miRNA maturation regulation [25]. We subsequently verified the results of RNA pulldown using Western blotting (Fig. 3B) and confirmed the binding relationship between CBX8 and pre-miR-127 through RIP assay (Fig. 3C). β -elemene treatment resulted in a significant downregulation of CBX8 expression (Fig. 3D), indicating that β -elemene affects CBX8 expression, which in turn influences the maturation of pre-miR-127. We further analyzed the CBX8 common motif region present in pre-miR-127 and designed corresponding mutant sequences (designated as pre-miR-127-WT or pre-miR-127-Mut) (Fig. 3E). The results of RNA pulldown-Western blot also confirmed the binding of pre-miR-127 to CBX8 at these sites (Fig. 3F), elucidating the binding relationship between the RNA-binding domain of CBX8 and pre-miR-127. Overexpression of CBX8 (Fig. 3G) was followed by the detection of related gene expression, which revealed that CBX8 positively regulates pre-miR-127, while negatively regulating miR-127-3p (Fig. 3H), consistent with the previously described function of CBX8 in restricting the nucleoplasmic transport of pre-miR-127 and inhibiting its transition to mature miR-127-3p (Figs. 3I and J). Under these circumstances, the binding of pre-miR-127 to DICER significantly decreased with excessive CBX8 (Fig. 3K).

The mechanism of miR-127-3p upregulation by β -elemene has been established, and the rescue experiments further validate this mechanism (Fig. S5). β -elemene inhibits CBX8, allowing pre-miR-127 to evade nucleoplasmic translocation restrictions, thereby promoting the maturation of pre-miR-127 to miR-127-3p and upregulating miR-127-3p expression.

3.4. β -Elemene regulates exosomal sorting of miR-127-3p by promoting SYNCRIP expression

The TME is a primary focus of our research, with a particular emphasis on macrophages, which are the most abundant immune cells in this environment. Consequently, we have investigated the potential role of β -elemene in modulating the TME. We conducted a comprehensive analysis of miR-127-3p expression in four groups of exosome samples (Fig. S6A) and performed detailed characterization of the exosomes (Figs. S6B and C). Interestingly, we observed a high expression of miR-127-3p in the exosomes derived from β -elemene-treated NSCLCs. This observation prompted us to further explore the relationship between β -elemene, miR-127-3p, and macrophages in our subsequent studies.

In the initial phase, we conducted RIP assays to screen 12 proteins involved in the regulation of RNA encapsulation into extracellular vesicles in two exosome samples [26]. miR-127-3p was found to be predominantly enriched in HNRNPC, HNRNPK, SYNCRIP, and MVP (Fig. S7A), while only SYNCRIP showed regulation by β -elemene (Figs. 4A and S7B). We observed that β -elemene promotes SYNCRIP expression, and this effect is attenuated when SYNCRIP is disrupted (Figs. S7C and D). Subsequently, we analyzed the binding of SYNCRIP to miR-127-3p in NSCLCs, and the results were consistent (Fig. 4B). Additionally, the expression of SYNCRIP significantly decreased after mutating miR-127-3p (Fig. 4C). Upon overexpression of SYNCRIP (Fig. 4D), the RT-qPCR results showed no significant change in miR-127-3p expression in NSCLCs, while miR-127-3p expression in exosomes was significantly elevated (Fig. 4E), suggesting that SYNCRIP promotes the packaging of miR-127-3p into exosomes.

groups, including differences in volume and weight, were shown. (E) Quantitative real-time polymerase chain reaction (RT-qPCR) analysis was performed to determine the expression of miR-127-3p in transplanted tumors obtained from different groups. (F) Immunohistochemistry (IHC) was used to detect the expression differences of cell proliferation marker Ki67, autophagy marker LC3, and macrophage M1 polarization marker CD86 in transplanted tumors from different sources. (G) Western blot analysis was conducted to examine the expression of autophagy-related proteins in transplanted tumors. All experimental groups in Figs. 6A–G were derived from the following four groups: PBS, β -elemene, β -elemene + NC antagonist, and β -elemene + miR-127-3p antagonist. After transfecting A549 cells for four weeks, the mice were weighed and the transplanted tumors were collected for subsequent experiments and analysis. PBS: phosphate-buffered saline; NC: negative control. ** $P < 0.01$.

To further validate the aforementioned mechanism, we employed RIP assays to assess the enrichment of miR-127-3p by SYNCRIP (Fig. 4F). We observed that β -elemene induced an upregulation of SYNCRIP, resulting in a greater enrichment of miR-127-3p. Conversely, overexpression of CBX8 led to a decrease in miR-127-3p expression, consequently reducing its enrichment. Correspondingly, RT-qPCR analysis detected changes in miR-127-3p expression under different treatments (Fig. 4G). In comparison to the group treated with β -elemene alone, interference with SYNCRIP after β -elemene treatment did not yield a significant difference in miR-127-3p expression. However, treatment involving CBX8 led to a significant decrease in miR-127-3p expression. Additionally, we performed a separate analysis of miR-127-3p expression in exosomes (Fig. 4H). In contrast to Fig. 4G, the regulation of miR-127-3p in exosomes was found to be simultaneous by with SYNCRIP and CBX8.

In conclusion, β -elemene upregulates SYNCRIP expression, which facilitates the packaging of miR-127-3p into exosomes.

3.5. β -elemene promotes macrophage polarization toward M1 by packaging and delivering miR-127-3p through NSCLCs-derived exosomes

The results of the study reveal a significant increase in the expression of miR-127-3p in exosomes derived from NSCLCs under the influence of β -elemene. To further investigate the relationship between β -elemene, miR-127-3p, and macrophages, a co-culture experiment combining NSCLCs-derived exosomes with macrophages was conducted. The findings clearly demonstrate the efficient uptake capacity of macrophages towards exosomes, as the exosomes predominantly enter the macrophages after a specific duration of co-culture (Fig. 5A). Subsequently, using RT-qPCR, a significant upregulation of miR-127-3p expression was detected in both macrophages co-cultured with β -elemene-treated NSCLCs and macrophages co-cultured with exosomes from β -elemene-treated NSCLCs (Fig. 5B).

Existing reports and the results presented in this study consistently demonstrate the anti-cancer properties of miR-127-3p. Therefore, the investigation focuses on whether miR-127-3p has the potential to induce macrophage polarization towards the M1 phenotype. Flow cytometry results indicate a significant increase in CD86-positive cells in β -elemene-treated NSCLCs or their secreted exosomes co-cultured with macrophages. This phenomenon was reversed after the addition of miR-127-3p antagonists (Fig. 5C). RT-qPCR was further used to detect the expression of M1 polarization markers in corresponding macrophages, and the results were consistent (Fig. 5D). These findings suggest that miR-127-3p induces macrophages towards M1 polarization. Further exploration is needed to understand the underlying reasons. Potential targets of miR-127-3p were predicted from miRDB (<https://mirdb.org/>) (Table 1), among which ZC3H4 showed significant downregulation in M1 macrophages compared to M0 macrophages ($P_{\text{Val}} < 0.05$, $\log_{2}\text{FC} < -1.0$), according to the data in the GSE69607 dataset (Fig. 5E). RT-qPCR analysis demonstrated that miR-127-3p negatively regulates ZC3H4 (Fig. 5F). The promoting role of ZC3H4 knockdown in regulating M1 polarization was validated by flow cytometry and RT-qPCR (Figs. 5G and H).

In conclusion, in the presence of β -elemene, NSCLCs deliver miR-127-3p via exosomes, which then inhibits ZC3H4 expression, promoting macrophage M1 polarization.

3.6. β -elemene-mediated miR-127-3p upregulation to inhibit NSCLC tumor growth *in vivo*

To validate the inhibitory effects of β -elemene on NSCLC tumor growth *in vivo*, a total of 20 nude mice were divided into four

groups: PBS, β -elemene, β -elemene + NC antagomir, and β -elemene + miR-127-3p antagomir. After a period of 28 days, the body weight of mice in each group was measured (Fig. 6A). Remarkably, the results of tumor volume and weight demonstrated that β -elemene treatment significantly suppressed tumor growth (Figs. 6B–D), and this inhibition was reversed when miR-127-3p was silenced. Subsequently, tumor tissues were isolated from each group of mice and subjected to various assays to confirm the function of β -elemene. The expression of miR-127-3p was assessed using RT-qPCR (Fig. 6E), and the results showed an opposite trend compared to tumor growth. Immunohistochemical staining and Western blot analysis revealed that β -elemene could inhibit proliferation, induce autophagy, and promote M1 polarization of macrophages, all of which were restored upon interference with miR-127-3p (Figs. 6F and G).

In conclusion, the findings suggest that β -elemene-mediated upregulation of miR-127-3p decelerates the growth of NSCLC tumors.

4. Discussion

In traditional Chinese medicine, β -elemene, an active compound isolated from *Curcuma wenyujin*, has been widely studied for its broad-spectrum anti-cancer properties and its potential use in the treatment of various types of cancer [8,27,28]. Previous studies have shown that β -elemene can regulate cancer cell progression through multiple pathways, including apoptosis induction, autophagy modulation, signaling pathway regulation, and cell cycle blockade, among others [29]. Additionally, β -elemene has been found to affect the content of exosomes, thereby inhibiting tumor cell drug resistance through the exosome pathway [30]. In this study, we conducted *in vitro* and *in vivo* experiments to investigate the mechanism of β -elemene in NSCLC from two perspectives: autophagy induction and the relationship between exosomes and macrophages.

β -elemene has been implicated in the occurrence and development of cancer through the induction of autophagy [31]. Our findings demonstrate that β -elemene treatment activates autophagy in NSCLCs, leading to reduced proliferation and increased apoptosis, indicating that β -elemene inhibits the occurrence and development of NSCLC by inducing autophagy. We focused on the MAPK/mTOR pathway, as MAPK4 has been shown to atypically activate the Akt/mTOR pathway [32]. Examination of β -elemene-treated NSCLCs revealed the inhibition of both MAPK4 and key factors of the Akt/mTOR pathway, providing a specific mechanism for autophagy activation. Bioinformatics analysis and mechanistic experiments further elucidated that miR-127-3p, which binds to the 3'UTR of MAPK4 and silences its expression, acts as an upstream regulator of MAPK4.

The maturation of miRNA is primarily regulated by the intracellular Drosha complex and DICER complex [33]. In NSCLCs treated with β -elemene, pre-miR-127 is released from its nuclear localization restriction due to decreased CBX8 expression, promoting the production of mature miR-127-3p. This confirms that the binding of CBX8 to pre-miRNA can regulate miRNA maturation [25]. The tumor-suppressing role of miR-127-3p has been widely reported in various cancers, including prostate cancer, oral squamous cell carcinoma, and osteosarcoma [33–35]. In our study, β -elemene indirectly contributed to the inhibition of NSCLC development through high expression of miR-127-3p.

Contrary to the expected inhibitory effect of β -elemene on exosome production [30], our study found that β -elemene can promote the upregulation of SYNCRIP expression. SYNCRIP is an important protein involved in exosomal miRNA sorting, and it facilitates the packaging of miR-127-3p into exosomes, which are

then delivered to macrophages, inducing a cancer-suppressing phenotype. Previous studies have shown that β -elemene can exert anti-tumor effects by modulating the tumor inflammatory environment and TME [36], and reports have indicated that miR-127-5p promotes M1 polarization in related diseases such as pneumonia [37,38]. In our study, we observed that macrophages displayed an M1 polarized phenotype under β -elemene treatment. ZC3H4, a protein associated with macrophage activation [39], was significantly downregulated in M1 macrophages compared to M0 macrophages according to the GSE69607 dataset. After interfering with ZC3H4, macrophages underwent M1 polarization. Our study revealed that miR-127-3p can negatively regulate the expression of ZC3H4, and similarly, macrophages exhibited M1 polarization after miR-127-3p infection. In summary, β -elemene induced the packaging and delivery of miR-127-3p into exosomes, which in turn inhibited ZC3H4 expression and promoted M1 polarization in macrophages.

Numerous *in vivo* experiments have confirmed the inhibitory effect of β -elemene on tumor growth. Chen et al. [40] demonstrated weaker tumor tissue fluorescence signals and reduced lymph node metastasis in a β -elemene-treated mouse model compared to the control group. Zhai et al. [41] found that the tumor size was significantly smaller in a bladder cancer xenograft mouse model after β -elemene treatment compared to the control group, with no significant changes in mouse body weight. These findings are consistent with our results. The tumors in xenograft mice treated with β -elemene exhibited significant reduction, while the body weight of the mice remained unaffected. However, this inhibitory effect was lost after interference with miR-127-3p. β -elemene treatment activated the expression of miR-127-3p, autophagy-related proteins, and M1 polarization markers, while inhibiting the expression of proliferation markers. These changes were reversed after interference with miR-127-3p.

Although our study provides important preclinical evidence for the anti-tumor effects of β -elemene in NSCLC, further validation is required to assess its clinical efficacy and safety in NSCLC patients. A deeper understanding of the mechanisms of action of β -elemene will provide a theoretical basis for the study of its therapeutic effects and safety in NSCLC. Additionally, we will explore the potential of combining β -elemene with existing standard treatment regimens and combination strategies for NSCLC. If clinical benefits are confirmed, β -elemene could offer a valuable targeted therapy for this patient population. Collaboration between basic researchers and clinical oncologists will accelerate the transition of this compound from the laboratory to clinical settings. In conclusion, this study provides strong scientific evidence to support the clinical development of β -elemene for the treatment of NSCLC, although further validation is required.

5. Conclusions

In summary, our study sheds light on the underlying mechanism by which β -elemene exerts its anti-tumor effects in NSCLCs. Specifically, β -elemene promotes the maturation of miR-127-3p by suppressing CBX8 expression, resulting in increased levels of miR-127-3p. This upregulated miR-127-3p inhibits MAPK4, leading to the inactivation of the MAPK4/mTOR pathway and induction of autophagy in NSCLCs. Furthermore, β -elemene enhances SYNCRIP expression, facilitating the packaging and delivery of miR-127-3p to macrophages via exosomes. Once delivered to macrophages, miR-127-3p silences ZC3H4, a critical factor for M1 polarization. As a result, macrophages undergo M1 polarization.

In conclusion, β -elemene demonstrates inhibitory effects on the development and progression of NSCLC through multiple mechanisms, suggesting its potential as a future treatment option for

NSCLC. This study provides significant scientific evidence supporting the therapeutic application of β -elemene.

CRedit author statement

Xiahui Wu: Conceptualization, Validation, Formal analysis, Investigation, Data curation, Project administration; **Jie Wu:** Conceptualization, Formal analysis, Investigation, Data Curation; **Tingting Dai:** Conceptualization, Formal analysis, Data curation; **Qiangcheng Wang:** Methodology, Software, Visualization; **Shengjie Cai:** Methodology, Software, Visualization; **Xuehan Wei:** Visualization; **Jing Chen:** Writing – Original draft, Writing – Review & Editing, Supervision; **Ziyu Jiang:** Resources, Writing – Original draft, Writing – Review & Editing, Funding acquisition.

Declaration of competing interest

The authors declare no potential conflicts of interest.

Acknowledgments

This work was supported by the National Natural Science Foundation of China (Grant No.: 81973525), Traditional Chinese Medicine Development Project of Jiangsu Province (Grant No.: ZT202112).

Appendix A. Supplementary data

Supplementary data to this article can be found online at <https://doi.org/10.1016/j.jpha.2024.03.002>.

Reference

- [1] P. Chen, Y. Liu, Y. Wen, et al., Non-small cell lung cancer in China, *Cancer Commun. (Lond)* 42 (2022) 937–970.
- [2] R.L. Siegel, K.D. Miller, A. Jemal, et al., Cancer statistics, *CA Cancer J. Clin.* 67 (2021) 7–30.
- [3] W. Cao, H. Chen, Y. Yu, et al., Changing profiles of cancer burden worldwide and in China: A secondary analysis of the global cancer statistics 2020, *Chin. Med. J.* 134 (2021) 783–791.
- [4] H. Sung, J. Ferlay, R.L. Siegel, et al., Global cancer statistics 2020: GLOBOCAN estimates of incidence and mortality worldwide for 36 cancers in 185 countries, *CA Cancer J. Clin.* 71 (2021) 209–249.
- [5] H. Sun, H. Zhang, H. Cai, et al., Burden of lung cancer in China, 1990–2019: Findings from the global burden of disease study 2019, *Cancer Contr.* 30 (2023), 10732748231198749.
- [6] C.-M. Bao, B.-B. Li, Traditional Chinese Medicine enhances absorption of lung lesions in corona virus disease 2019 patient, *J. Tradit. Chin. Med.* 41 (2021) 982–984.
- [7] P. Wu, X. Dong, G. Song, et al., Bioactivity-guided discovery of quality control markers in rhizomes of *Curcuma wenyujin* based on spectrum-effect relationship against human lung cancer cells, *Phytomedicine* 86 (2021), 153559.
- [8] Z. Jiang, J.A. Jacob, D.S. Loganathachetti, et al., β -elemene: Mechanistic studies on cancer cell interaction and its chemosensitization effect, *Front. Pharmacol.* 8 (2017), 105.
- [9] Z. Jiang, S. Qin, X. Yin, et al., Synergistic effects of Endostar combined with β -elemene on malignant ascites in a mouse model, *Exp. Ther. Med.* 4 (2012) 277–284.
- [10] Y. Lei, E. Zhang, L. Bai, et al., Autophagy in cancer immunotherapy, *Cells* 11 (2022), 2996.
- [11] H. Morishita, N. Mizushima, Diverse cellular roles of autophagy, *Annu. Rev. Cell Dev. Biol.* 35 (2019) 453–475.
- [12] Q. Cao, X. You, L. Xu, et al., PAQR3 suppresses the growth of non-small cell lung cancer cells via modulation of EGFR-mediated autophagy, *Autophagy* 16 (2020) 1236–1247.
- [13] C. Xie, X. Zhou, C. Liang, et al., Apatinib triggers autophagic and apoptotic cell death via VEGFR2/STAT3/PD-L1 and ROS/Nrf2/p62 signaling in lung cancer, *J. Exp. Clin. Cancer Res.* 40 (2021), 266.
- [14] Z. Sun, K. Shi, S. Yang, et al., Effect of exosomal miRNA on cancer biology and clinical applications, *Mol. Cancer* 17 (2018), 147.
- [15] Z. Sun, S. Yang, Q. Zhou, et al., Emerging role of exosome-derived long non-coding RNAs in tumor microenvironment, *Mol. Cancer* 17 (2018), 82.
- [16] Z. Zhang, L. Xiong, L. Xue, et al., MiR-127-3p targeting CISD1 regulates autophagy in hypoxic-ischemic cortex, *Cell Death Dis.* 12 (2021), 279.
- [17] J. Cen, Y. Liang, Y. Huang, et al., Circular RNA circSDHC serves as a sponge for

- miR-127-3p to promote the proliferation and metastasis of renal cell carcinoma via the CDKN3/E2F1 axis, *Mol. Cancer* 20 (2021), 19.
- [18] B. Chen, M. Wang, R. Huang, et al., Circular RNA circLGMN facilitates glioblastoma progression by targeting miR-127-3p/LGMN axis, *Cancer Lett.* 522 (2021) 225–237.
- [19] P.J. Murray, Macrophage polarization, *Annu. Rev. Physiol.* 79 (2017) 541–566.
- [20] M. Allen, J. Louise Jones, Jekyll and Hyde: The role of the microenvironment on the progression of cancer, *J. Pathol.* 223 (2011) 162–176.
- [21] P.J. Murray, T.A. Wynn, Protective and pathogenic functions of macrophage subsets, *Nat. Rev. Immunol.* 11 (2011) 723–737.
- [22] X. Zhang, W. Liang, J. Liu, et al., Long non-coding RNA UFC1 promotes gastric cancer progression by regulating miR-498/Lin28b, *J. Exp. Clin. Cancer Res.* 37 (2018), 134.
- [23] Y. Liu, Z. Jiang, Y. Zhou, et al., β -elemene regulates endoplasmic reticulum stress to induce the apoptosis of NSCLC cells through PERK/IRE1 α /ATF6 pathway, *Biomed. Pharmacother.* 93 (2017) 490–497.
- [24] W. Wang, T. Shen, B. Dong, et al., MAPK4 overexpression promotes tumor progression via noncanonical activation of AKT/mTOR signaling, *J. Clin. Invest.* 129 (2019) 1015–1029.
- [25] X. Song, W. Ning, J. Niu, et al., CBX8 acts as an independent RNA-binding protein to regulate the maturation of miR-378a-3p in colon cancer cells, *Hum. Cell* 34 (2021) 515–529.
- [26] F. Fabbiano, J. Corsi, E. Gurrieri, et al., RNA packaging into extracellular vesicles: An orchestra of RNA-binding proteins? *J. Extracell. Vesicles* 10 (2020), e12043.
- [27] M. Gong, Y. Liu, J. Zhang, et al., β -elemene inhibits cell proliferation by regulating the expression and activity of topoisomerases I and II α in human hepatocarcinoma HepG-2 cells, *Biomed Res. Int.* 2015 (2015), 153987.
- [28] J. Zhang, H. Zhang, L. Chen, et al., β -elemene reverses chemoresistance of breast cancer via regulating MDR-related microRNA expression, *Cell. Physiol. Biochem.* 34 (2014) 2027–2037.
- [29] T. Tan, J. Li, R. Luo, et al., Recent advances in understanding the mechanisms of elemene in reversing drug resistance in tumor cells: A review, *Molecules* 26 (2021), 5792.
- [30] J. Zhang, H.-D. Zhang, Y.-F. Yao, et al., β -elemene reverses chemoresistance of breast cancer cells by reducing resistance transmission via exosomes, *Cell. Physiol. Biochem.* 36 (2015) 2274–2286.
- [31] S. Liu, Q. Li, G. Li, et al., The mechanism of m⁶A methyltransferase METTL3-mediated autophagy in reversing gefitinib resistance in NSCLC cells by β -elemene, *Cell Death Dis.* 11 (2020), 969.
- [32] Y. Liang, D. Zhu, L. Zhu, et al., Dichloroacetate overcomes oxaliplatin chemoresistance in colorectal cancer through the miR-543/PTEN/akt/mTOR pathway, *J. Cancer* 10 (2019) 6037–6047.
- [33] D. Wang, L. Tang, H. Wu, et al., miR-127-3p inhibits cell growth and invasiveness by targeting ITGA6 in human osteosarcoma, *IUBMB Life* 70 (2018) 411–419.
- [34] J. Fan, W. Du, H. Zhang, et al., Transcriptional downregulation of miR-127-3p by CTCF promotes prostate cancer bone metastasis by targeting PSMB5, *FEBS Lett.* 594 (2020) 466–476.
- [35] L. Ji, Z.N. Zhu, C.J. He, et al., miR-127-3p targets KIF3B to inhibit the development of oral squamous cell carcinoma, *Eur. Rev. Med. Pharmacol. Sci.* 23 (2019) 630–640.
- [36] Q. Xie, F. Li, L. Fang, et al., The antitumor efficacy of β -elemene by changing tumor inflammatory environment and tumor microenvironment, *Biomed Res. Int.* 2020 (2020), 6892961.
- [37] H. Ying, Y. Kang, H. Zhang, et al., miR-127 modulates macrophage polarization and promotes lung inflammation and injury by activating the JNK pathway, *J. Immunol.* 194 (2015) 1239–1251.
- [38] X. Liu, Y. Mao, Y. Kang, et al., microRNA-127 promotes anti-microbial host defense through restricting A20-mediated de-ubiquitination of STAT3, *iScience* 23 (2020), 100763.
- [39] X. Yang, J. Wang, Z. Zhou, et al., Silica-induced initiation of circular ZC3H4 RNA/ZC3H4 pathway promotes the pulmonary macrophage activation, *FASEB J.* 32 (2018) 3264–3277.
- [40] P. Chen, X. Li, R. Zhang, et al., Combinative treatment of β -elemene and cetuximab is sensitive to KRAS mutant colorectal cancer cells by inducing ferroptosis and inhibiting epithelial-mesenchymal transformation, *Theranostics* 10 (2020) 5107–5119.
- [41] B. Zhai, Q. Wu, W. Wang, et al., Preparation, characterization, pharmacokinetics and anticancer effects of PEGylated β -elemene liposomes, *Cancer Biol. Med.* 17 (2020) 60–75.